Optimization of Cancellation Path Model in Filtered-X LMS for Narrow Band Noise Suppression

Hyoun-Suk Kim and Youngjin Park

Abstract : Adaptive algorithms based on gradient adaptation have been extensively investigated and successfully joined with active noise/vibration control applications. The Filtered-X LMS algorithm became one of the basic feedforward algorithms in such applications, but is not fully understood yet. Effects of cancellation path model on the Filtered-X LMS algorithm have investigated and some useful properties related to stability were discovered. Most of the results stated that the error in the cancellation path model is undesirable to the Filtered X LMS. However, we started convergence analysis of Filtered-X LMS based on the assumption that erroneous model does not always degrade its performance. In this paper, we present a way of optimizing the cancellation path model in order to enhance the convergence speed by introducing intentional phase error. Carefully designed intentional phase error enhances the convergence speed of the Filtered-X LMS algorithm for pure tone noise suppression application without any performance loss at steady state.

Keywords : filtered-X LMS, active noise control, narrow band noise, eigenvalue spread

I. Introduction

Adaptive filters updated by the gradients of their cost function are widely used in active noise and vibration control applications. Among them, the Filtered-X LMS algorithm [1]-[3] that can cope with the systems having *cancellation path* - an auxiliary path between control speaker input and error microphone output - has been the most popular algorithm for its low computational burden and easy programming.

In ANC (Active Noise Control) system a reference signal measured from noise source is filtered through an adaptive filter. Its output is control signal and is fed to a secondary speaker. The weights of adaptive filter are updated to the direction of minimizing the instantaneous squared error measured from an error microphone. The update process requires prefiltering of the reference signal through the model of the cancellation path to ensure the stability of the update process. Allowable model error is confined only by the phase error between the actual cancellation path and its model. The limit of phase error is 90°[2]-[4].

If the degree of freedom of reference signal does not exceed that of the adaptive filter, i.e. *exact or underdetermined case*, the steady state weight values are independent of the model error providing that the phase error does not exceed 90°[4]. In this case, we have another design parameter - *phase error of cancellation path model* - whose allowable range is ±90°. This is independent of steady state performance. An example of the 'exact or underdetermined case' is narrow band noise suppression application where two adaptive weights are sufficient to deal with a pure tone reference signal. Here, we present a novel design procedure that primarily injects an *intentional phase error* to the cancellation path model to achieve fast convergence of the Filtered-X LMS algorithm.

Manuscript received : Aug. 24, 1998., Accepted : July. 5. 1999.
Hyoun Suk Kim : ETRI (Korea Electronics and Telecommunications Research Institute).
Youngjin Park : Korea Advanced Institute of Science and Technology.

II. Gradient description

The active control system using Filtered-X LMS we are concerning about is in Fig. 1. We assume that this system is excited with pure tone single reference input x_k of ω frequency and its output y_k is intended to cancel the primary noise at the error microphone location. W represents the adaptive filter, P the plant between the reference and the error microphone signal, and H and C the cancellation path and its model, respectively.

In Filtered-X LMS algorithm with only one frequency component ω in the reference, cost function J_k is defined as instantaneous squared error as follows:

$$J_k = e_k^2 = \bar{e}_k(\omega)e_k(\omega) \tag{1}$$

where $e_k(\omega)$ is Fourier transform of error signal e_k at the excitation frequency ω, and superscript - represents complex conjugate. Assuming slow change of weight

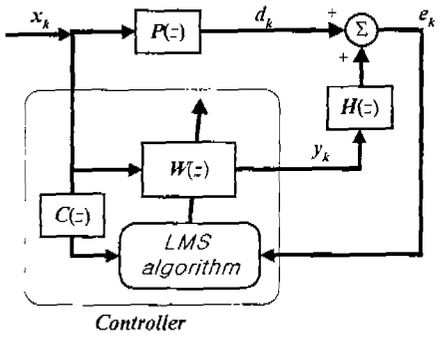

Fig. 1. Block diagram of ANC system.

values, from diagram of Fig. 1 we can express $e_k(\omega)$ as

$$e_k(\omega) = \{P(j\omega) + H(j\omega)W_k(j\omega)\}\, x_k(\omega) \tag{2}$$

where $P(j\omega)$, $H(j\omega)$ and $W_k(j\omega)$ are complex transfer functions at frequency ω of plant, cancellation path, and adaptive filter, respectively and $x_k(\omega)$ is Fourier transform of reference signal x_k. The exact formulation in time domain needs very complicated mathematics, so we assume slow change of weight values for simplicity and represent the error of (2) in the frequency domain.

Complex weight value at ω, $W_k(j\omega)$, can be expressed by conventional FIR type W_k of length $L+1$ and time to frequency domain transformation vector $Z_L(j\omega)$ of length $L+1$ as follows:

$$W_k(j\omega) = Z_L^t(j\omega)W_k \tag{3}$$

$$Z_L(j\omega) = \frac{1}{\sqrt{L+1}}\left[1 \;\; e^{-j\omega} \;\; e^{-j2\omega} \;\; \cdots \;\; e^{-jL\omega T}\right]^t \tag{4}$$

$$W = \left[w_0 \;\; w_1 \;\; w_2 \;\; \cdots \;\; w_L\right]^t \tag{5}$$

where $w_{i,k}$ is the i-th FIR coefficient of adaptive filter W at time step k, and T is sampling interval.

Using (2) and (3), differentiation of cost function J_k with respect to W_k gives true instantaneous gradient vector ∇W_k in time domain as

$$\nabla W_k = 2\,\mathrm{Re}\{H(j\omega)Z_L(j\omega)x_k(\omega)\overline{e}_k(\omega)\}. \tag{6}$$

Since we should use estimated cancellation path model C instead of true cancellation path H in the gradient calculation, the estimated gradient is

$$\begin{aligned}\hat{\nabla}W_k &= 2\,\mathrm{Re}\{C(j\omega)Z_L(j\omega)x_k(\omega)\overline{e}_k(j\omega)\}\\ &= 2\,\mathrm{Re}\{Z_L(j\omega)\overline{H}(j\omega)C(j\omega)\overline{Z}_L^t(j\omega)\}|x_k(\omega)|^2 W_k\\ &\quad +2\,\mathrm{Re}\{Z_L(j\omega)C(j\omega)\overline{P}(j\omega)\}|x_k(\omega)|^2\end{aligned} \tag{7}$$

For further investigation, let's express the prescribed transfer functions in terms of real and imaginary part as follows:

$$Z_L(j\omega) = Z_{Lx} + jZ_{Ly} \tag{8.a}$$

$$P(j\omega) = p\cos\phi_p + jp\sin\phi_p \tag{8.b}$$

$$C(j\omega) = c\cos\phi_c + jc\sin\phi_c \tag{8.c}$$

$$H(j\omega) = h\cos\phi_h + jh\sin\phi_h \tag{8.d}$$

where p, c, and h are magnitudes and ϕ_p, ϕ_c, and ϕ_h are phases of relevant transfer functions. Using (8), estimated gradient in (7) can be rewritten in a matrix equation (see Appendix A for details)

$$\hat{\nabla}W_k = 2\{\boldsymbol{S}_L\boldsymbol{H}^t\boldsymbol{C}\boldsymbol{S}_L^t\}W_k + 2\{\boldsymbol{S}_L\boldsymbol{C}\boldsymbol{P}\} \tag{9}$$

where matrices $\boldsymbol{S}_L$, $\boldsymbol{H}$, $\boldsymbol{C}$, and vector P are defined as follows:

$$\boldsymbol{S}_L = \left[Z_{Lx} \;\; Z_{Ly}\right] \tag{10.a}$$

$$\boldsymbol{H} = qh\begin{bmatrix}\cos\phi_h & \sin\phi_h\\ -\sin\phi_h & \cos\phi_h\end{bmatrix} \tag{10.b}$$

$$\boldsymbol{C} = qc\begin{bmatrix}\cos\phi_c & \sin\phi_c\\ -\sin\phi_c & \cos\phi_c\end{bmatrix} \tag{10.c}$$

$$P = qp\begin{bmatrix}\cos\phi_p\\ \sin\phi_p\end{bmatrix} \tag{10.d}$$

$$q = |x_k(\omega)| \tag{10.e}$$

Note that 2 by 2 matrices $\boldsymbol{H}$ and $\boldsymbol{C}$ are rotation matrices of angles $-\phi_h$ and $-\phi_c$, respectively. The matrix $\boldsymbol{K} = \boldsymbol{S}_L\boldsymbol{H}^t\boldsymbol{C}\boldsymbol{S}_L^t$ in (9) is *cross correlation matrix* of the two filtered reference signals through H and C. This matrix is very important in the convergence process. Let's denote the cross-correlation matrix as $\boldsymbol{K}$.

$$\boldsymbol{K} = \boldsymbol{S}_L\boldsymbol{H}^t\boldsymbol{C}\boldsymbol{S}_L^t \text{ ; cross-correlation matrix.} \tag{11}$$

Let's introduce a parameter θ representing the phase difference between $H(j\omega)$ and $C(j\omega)$, then from (10) $\boldsymbol{H}^t\boldsymbol{C}$ term in matrix $\boldsymbol{K}$ is rearranged in terms of θ as follows:

$$\theta = \phi_c - \phi_h \tag{12}$$

$$\boldsymbol{H}^t\boldsymbol{C} = q^2hc\begin{bmatrix}\cos\theta & \sin\theta\\ -\sin\theta & \cos\theta\end{bmatrix} \tag{13}$$

Note that $\boldsymbol{H}^t\boldsymbol{C}$ is a rotation matrix of angle $-\theta$ which causes unsymmetricity of $\boldsymbol{K}$. If $\theta = 0$, $\boldsymbol{K}$ becomes proportional to auto-correlation matrix of filtered reference signal.

III. Decomposition of K

Cross-correlation matrix $\boldsymbol{K}$ can be decomposed into the following form (see Appendix B for details)

$$\boldsymbol{K} = \boldsymbol{U}_L\boldsymbol{Q}\Lambda\boldsymbol{Q}^{-1}\boldsymbol{U}_L^t \tag{14}$$

where $L+1$ by 2 matrix $\boldsymbol{U}_L$ is column space of $\boldsymbol{S}_L$ satisfying $\boldsymbol{U}_L^t\boldsymbol{U}_L = \boldsymbol{I}$, Λ is 2 by 2 diagonal matrix having eigenvalues of $\boldsymbol{K}$ on its diagonal parts, and $\boldsymbol{Q}$ is 2 by 2 invertable matrix. Their detailed expressions are as follows:

$$\boldsymbol{U}_L = \boldsymbol{B}_L\Sigma_L^{-1} \tag{15.a}$$

$$\boldsymbol{Q} = \left(\alpha_L\cos\theta + \sqrt{1-\alpha_L^2}\sin\theta\right)\begin{bmatrix}1 & 1\\ 1 & 1\end{bmatrix} + \beta_L\begin{bmatrix}1 & -1\\ -1 & 1\end{bmatrix}$$

$$\Lambda = diag[\lambda_1, \lambda_2] \tag{15.b}$$

$$= \tfrac{1}{2}q^2hc\cos\theta\begin{bmatrix}1+\dfrac{\beta_L}{|\cos\theta|} & 0\\ 0 & 1-\dfrac{\beta_L}{|\cos\theta|}\end{bmatrix} \tag{15.c}$$

where B_L, Σ_L, α_L, and β_L are defined as follows:

$$B_L = \frac{1}{\sqrt{L+1}} \begin{bmatrix} \cos\frac{1}{2}\omega T & \sin\frac{1}{2}\omega T \\ \cos(\frac{1}{2}-1)\omega T & \sin(\frac{1}{2}-1)\omega T \\ \vdots & \vdots \\ \cos(\frac{1}{2}-1)\omega T & -\sin(\frac{1}{2}-1)\omega T \\ \cos\frac{1}{2}\omega T & -\sin\frac{1}{2}\omega T \end{bmatrix} \quad (16.a)$$

$$\Sigma_L = \begin{bmatrix} \sqrt{\frac{1+\alpha_L}{2}} & 0 \\ 0 & \sqrt{\frac{1-\alpha_L}{2}} \end{bmatrix} \quad (16.b)$$

$$\alpha_L = \frac{\sin(L+1)\omega T}{(L+1)\sin\omega T} \quad (16.c)$$

$$\beta_L = \sqrt{\alpha_L^2 - \sin^2\theta} \quad (16.d)$$

The variable α_L is a function of filter length L+1 and ωT. Note that ωT is 2π times of normalized target frequency f/f_s, *i.e.* $\omega T = 2\pi f/f_s$.

Using (9), (11) and (14) update equation of Filtered-X LMS algorithm; $W_{k+1}=W_k-\mu\hat{\nabla}W_k$ can be rewritten in modal domain weight vector $Q^{-1}U^t{}_LW$ as follows

$$(Q^{-1}U_L^tW_{k+1}) = [1-2\mu\Lambda](Q^{-1}U_L^tW_k) - 2\mu Q^{-1}U_L^tS_LCP \quad (17)$$

Clearly, the convergence characteristics depend on eigenvalues in Λ as well as the convergence parameter μ, though the eigenvectors (the columns of U_LQ) may not orthogonal for non-zero value of θ. From (15.c), the real parts of the two eigenvalues become negative when $|\theta|$ exceeds 90° which implies the algorithm is unstable for any positive μ.

IV. Eigenvalue spread

The convergence speed can be controlled to some extent by the convergence parameter μ, but maximum attainable speed is limited by the eigenvalue spread of K. If the eigenvalue spread is unity, fastest convergence is possible. So it is reasonable to state that the convergence speed is mainly determined by the 'eigenvalue spread' of K.

At most, only two eigenvalues of K are non-zero for a pure tone reference input. Also, two eigenvalues of K are expected to be dominant for narrow band reference input. In this section, the spread of the two eigenvalues will be given in terms of some design parameters. By investigating the parameters included in eigenvalue spread, some conditions that make it unity can be found.

From (15.c) the eigenvalue spread r is

$$r = \frac{|\cos\theta|+\beta_L}{|\cos\theta|-\beta_L} \quad (18)$$

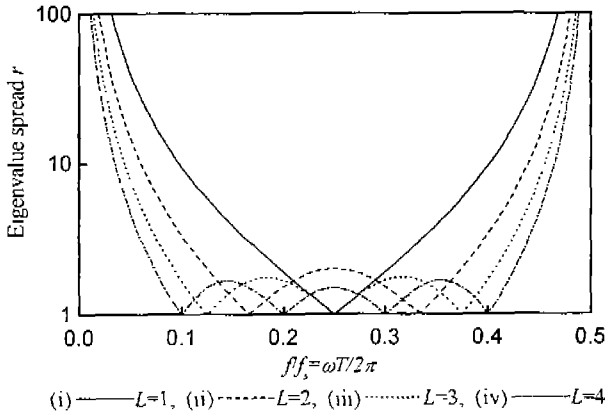

Fig. 2. Eigenvalue spread along f/fs with $\theta = 0$.

The resulting eigenvalue spread depends on three parameters; the model phase error θ, the adaptive filter length L+1, and the normalized target frequency f/f_s. Fig. 2 shows eigenvalue spread r when $\theta = 0$ along the normalized target frequency f/f_s using (18) with $L = 1, 2, 3, 4$. This illustrates some useful properties. For example, if $L = 1$, *i.e.* with two adaptive coefficients, eigenvalue spread becomes minimum and the convergence speed can be maximized if the sampling frequency is two times of the target frequency. Also, on can see that as filter length increases, the eigenvalue spread is lowered in average sense. Thus, qualitatively it can be said that the long filter length can increase the convergence speed for arbitrary f/f_s.

Eigenvalue spread r becomes its minimum, unity, when $\beta_L = 0$. From (16.d) this implies

$$\sin^2\theta = \alpha_L^2 \quad (19)$$

Using the value α_L defined in (16.c), optimum model error θ_{opt} for fast convergence is determined as follows

$$\theta_{opt} = \pm\sin^{-1}\left[\frac{\sin(L+1)\omega T}{(L+1)\sin\omega T}\right] \quad (20)$$

Note that there are two values of θ_{opt} whose absolute values are equal to each other. If $\theta_{opt} = 0$, there needs no extra effort to increase convergence speed; exact phase model gives the eigenvalue spread unity.

Fig. 3 shows $|\theta_{opt}|$ along f/f_s using (20) with $L = 1$, 2, 3, 4. Zero θ_{opt} occurs when $\sin(L+1)\omega T$ is zero, i.e. normalized target frequency f/f_s is equal to $k/2(L+1)$ for $k = 1, 2, \cdots, L$. The L points when $\theta_{opt} = 0$ satisfies $r = 1$. If we could set f/f_s to one of these values by adjusting f_s, no modification of exact cancellation path model is necessary for faster convergence. If the adjustment of f_s is not allowed, introduction of optimal phase error θ_{opt} could give faster convergence. This will be discussed in detail in following section. Another way to make θ_{opt} near zero is increasing L.

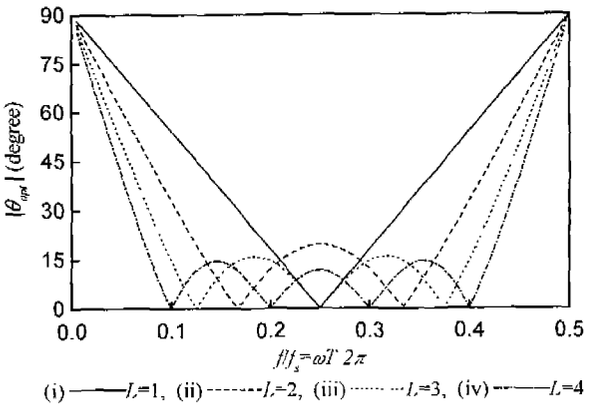

Fig. 3. $|\theta_{opt}|$ along f/f_s.

However, this increases computational burden in the real-time process.

V. Optimum model design

We will now describe how the cancellation path model can be modified to get fast convergence. We assume that cancellation path model C is FIR type with $M+1$ taps and is estimated prior to implementing Filtered-X LMS so that it can be said 'exact' around the known target frequency ω. This model can be obtained by exciting the cancellation path with periodic signal containing periodic signal of frequency ω.

$$C=[c_0 \quad c_1 \quad \cdots \quad c_M]^t \text{; accurate model of H at } \omega \qquad (21)$$

A transformation matrix $\boldsymbol{F}$ through which optimal cancellation path C_{opt} can be calculated from C will be presented. The desired mathematical expression is

$$C_{opt} = \boldsymbol{F}C \qquad (22)$$

Let's denote that $C_{opt}(j\omega)$ is the frequency response of $C_{opt}(z)$ at ω. Providing that $C(j\omega)$ is equal to $H(j\omega)$, the phase difference between $C_{opt}(j\omega)$ and $C(j\omega)$ must be θ_{opt}, *i.e.*

$$C_{opt}(j\omega) = e^{j\theta_{opt}} C(j\omega) \qquad (23)$$

A equivalent matrix expression is

$$\begin{bmatrix} Z'_{Mx} \\ Z'_{My} \end{bmatrix} C_{opt} = \begin{bmatrix} \cos\theta_{opt} & -\sin\theta_{opt} \\ \sin\theta_{opt} & \cos\theta_{opt} \end{bmatrix} \begin{bmatrix} Z'_{Mx} \\ Z'_{My} \end{bmatrix} C \qquad (24)$$

Comparing (22) and (24), the transformation matrix $\boldsymbol{F}$ is

$$\boldsymbol{F} = \begin{bmatrix} Z'_{Mx} \\ Z'_{My} \end{bmatrix}^{+} \begin{bmatrix} \cos\theta_{opt} & -\sin\theta_{opt} \\ \sin\theta_{opt} & \cos\theta_{opt} \end{bmatrix} \begin{bmatrix} Z'_{Mx} \\ Z'_{My} \end{bmatrix} \qquad (25)$$

where superscript $^+$ is pseudo inverse. Noting that from (10.a) $[Z_{Mx}\ Z_{My}]$ is $\boldsymbol{S}_M$, and using (15.a) and (A.1), $\boldsymbol{F}$ becomes

$$\boldsymbol{F} = \boldsymbol{B}_M \boldsymbol{\Sigma}_M^{-2} \begin{bmatrix} \cos\theta_{opt} & -\sin\theta_{opt} \\ \sin\theta_{opt} & \cos\theta_{opt} \end{bmatrix} \boldsymbol{B}_M^t \qquad (26)$$

where two matrices $\boldsymbol{B}_M$ and $\boldsymbol{\Sigma}_M$ are in (16.a) and (16.b), respectively.

Overall procedure of getting C_{opt} can be summarized as follows.

1. Obtain C by modeling the cancellation path.
1. Select adaptive filter length $L+1$ and $\omega T(=2\pi f/f_s)$.
3. Calculate θ_{opt} from (20).
4. Calculate $\boldsymbol{F}$ from (26)
5. Calculate C_{opt} from (22).

Replacing the $C(z)$ with $C_{opt}(z)$ in the Filtered-X LMS algorithms of Fig. 1, faster convergence speed becomes possible.

VI. Computer simulations

In computer simulation, adaptive weight length is set to 2, *i.e.*, $W(z)=w_0+w_1z^{-1}$, and the plant $P(z)$ and cancellation path $H(z)$ are chosen as follows

$$P(z) = 0.3z^{-6} + z^{-7} + 2z^{-8} + z^{-9} + 0.1z^{-10}$$
$$H(z) = z^{-4} + 2z^{-5} \ (i.e.\ H=[0\ 0\ 0\ 0\ 1\ 2]^t)$$

We chose 30% of maximum stable μ for all cases and injected white noise at e_k whose variance is $(10^{-12})/3$ to make it the desired cost function at steady state. Fig. 4 shows time domain squared error and weight trajectories when $f/f_s=0.2$ for (a) conventional C, (b) C_{opt} using $|\theta_{opt}|$, (c) C_{opt} using $-|\theta_{opt}|$. Fig. 5 and Fig. 6 show the same when $f/f_s=0.4$ and $f/f_s=0.8$, respectively.

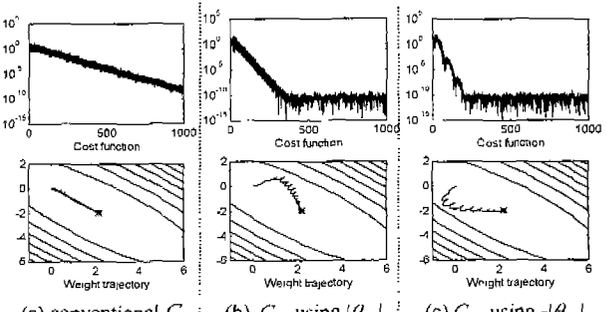

Fig. 4. Cost function J_k and weight trajectory (w_0,w_1) when $f/f_s=0.2$ ($|\theta_{opt}|=54°$). (* : optimum weight)

Computer simulations including proposed optimum cancellation path model C_{opt} using $|\theta_{opt}|$ or $-|\theta_{opt}|$ leads faster convergence of the cost function than the case using exact model. The optimum cancellation path increases the convergence speed more for the case of smaller r in non-optimized situation. The weight trajectory is distorted if the phase error is introduced to modify C. This trajectory is closely related with the right eigenvectors of $\boldsymbol{K}$, *i.e.* the

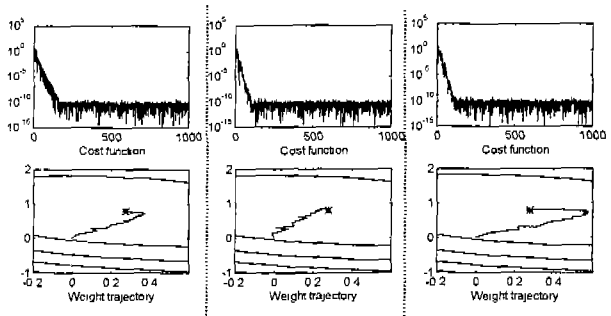

(a) conventional C $r = 0.5279$ $\mu = 0.0109$ (b) C_{opt} using $|\theta_{opt}|$ $r = 1$ $\mu = 0.0124$ (c) C_{opt} using $-|\theta_{opt}|$ $r = 1$ $\mu = 0.0138$

Fig. 5. Cost function J_k and weight trajectory (w_0, w_1) when $f/f_s = 0.4$ ($|\theta_{opt}| = 18°$). (* : optimum weight)

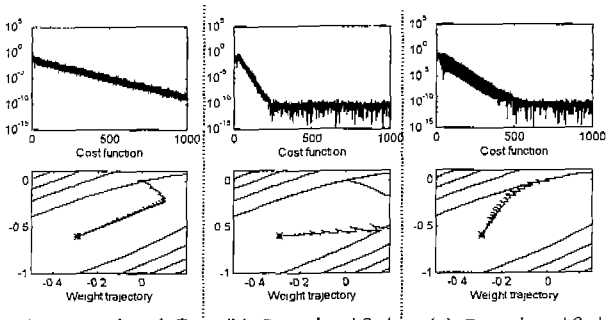

(a) conventional C $r = 0.1056$ $\mu = 0.0230$ (b) C_{opt} using $|\theta_{opt}|$ $r = 1$ $\mu = 0.0490$ (c) C_{opt} using $-|\theta_{opt}|$ $r = 1$ $\mu = 0.0263$

Fig. 6. Cost function J_k and weight trajectory (w_0, w_1) when $f/f_s = 0.8$ ($|\theta_{opt}| = 54°$). (* : optimum weight)

columns of $\boldsymbol{U}_k\boldsymbol{Q}$. It is interesting that the shape of the trajectories have no relation to the convergence speed as shown in the simulation results. The starting directions of trajectories when using $|\theta_{opt}|$ and $-|\theta_{opt}|$ are in opposite side with respect to that of the conventional case.

VI. Conclusions

A method of modifying cancellation path model to increase the convergence speed of the Filtered-X LMS algorithm for narrow-band noise suppression application was presented. Presented method inserts intentional phase error to the cancellation path model that is originally well estimated around the target frequency. The intentional phase error was optimally calculated to lower the eigenvalue spread to its minimum. Some illustrative examples verified the proposed framework to speed up the convergence of Filtered-X LMS.

Obtained convergence characteristic is similar to LS method that uses inversion of correlation matrix because the eigenvalue spread is adjusted to unity. The merit of proposed method compared to LS method is that there is no increase in computational load in real-time application because modifying the model can be done prior to control stage.

References

[1] B. Widrow, S. D. Stearns, "Adaptive signal processing," Prentice-Hall. Ic. 1985.

[2] S. D. Snyder, C. H. Hansen, "The influence of transducer transfer functions and acoustic time delays on the implementation of the LMS algorithm in active noise control system," *Journal of Sound and Vibration*, vol. 141, no. 3, pp. 409-424. 1990.

[3] S. D. Snyder and C. H. Hansen, "The effects of transfer function estimation errors on the Filtered-X LMS algorithm," IEEE, SP, vol. 42, no. 4, pp. 950-953. 1994.

[4] H. S. Kim, Y. Park, "Delayed-X LMS algorithm : an efficient ANC algorithm utilizing the robustness of cancellation path model," *Journal of Sound and Vibration*, vol. 212, no. 5, pp. 875-887, 1998.

Appendix A: Derivation form (7) to (9)

The derivation consists of proofs of following two equalities

$$\mathrm{Re}\left\{Z_i(j\omega)\overline{H}(j\omega)C(j\omega)\overline{Z}_i'(j\omega)\right\}q^2 = \boldsymbol{S}_i\boldsymbol{H}'\boldsymbol{C}\boldsymbol{S}_i' \quad \text{(A.1)}$$

$$\mathrm{Re}\left\{Z_i(j\omega)C(j\omega)\overline{P}(j\omega)\right\}q^2 = \boldsymbol{S}_L\boldsymbol{C}\boldsymbol{P} \quad \text{(A.2)}$$

1. Proof of (A.1)

Let's denote $\overline{H}(j\omega)C(j\omega) = a_x + ja_y$, then the left-hand side of (A.1) can be arranged as follows:

$$\begin{aligned}
&\mathrm{Re}\left\{Z_i(j\omega)\overline{H}(j\omega)C(j\omega)\overline{Z}_i'(j\omega)\right\}q^2 \\
&= \mathrm{Re}\left\{(Z_{ix} + jZ_{iy})(a_x + ja_y)(Z_{ix}' + jZ_{iy}')\right\}q^2 \\
&= \left\{a_x(Z_{ix}Z_{ix}' + Z_{iy}Z_{iy}') + a_y(Z_{ix}Z_{iy}' - Z_{iy}Z_{ix}')\right\}q^2 \\
&= \begin{bmatrix} Z_{ix} & Z_{iy} \end{bmatrix}\begin{bmatrix} a_x & a_y \\ -a_y & a_x \end{bmatrix}\begin{bmatrix} Z_{ix}' \\ Z_{iy}' \end{bmatrix}q^2
\end{aligned} \quad \text{(A.3)}$$

Denoting h_x and h_y as real and complex parts of $H(j\omega)$, and c_x and c_y as real and imaginary parts of $C(j\omega)$, also as we denoted $\overline{H}(j\omega)C(j\omega) = a_x + ja_y$, a_x and a_y becomes

$$a_x = h_x c_x + h_y c_y \quad \text{(A.4)}$$

$$a_y = h_x c_y - h_y c_x \quad \text{(A.5)}$$

Thus, the 2 by 2 matrix in (A-3) is

$$\begin{aligned}
\begin{bmatrix} a_x & a_y \\ -a_y & a_x \end{bmatrix} &= \begin{bmatrix} h_x c_x + h_y c_y & h_x c_y - h_y c_x \\ -h_x c_y + h_y c_x & h_x c_x + h_y c_y \end{bmatrix} \\
&= \begin{bmatrix} h_x & -h_y \\ h_y & h_x \end{bmatrix}\begin{bmatrix} c_x & c_y \\ -c_y & c_x \end{bmatrix}
\end{aligned} \quad \text{(A.6)}$$

From (A.3), (A.6), and using the definitions of (10.a)-(10.e), the proof of equality (A.1) is straightforward.

2. Proof of (A.2)

Let's denote $C(j\omega)\overline{P}(j\omega) = b_x + jb_y$, then the left-hand side of (A.2) can be arranged as follows:

$$\begin{aligned}&\mathrm{Re}\{Z_L(j\omega)C(j\omega)\overline{P}(j\omega)\}q^2\\&= \mathrm{Re}\{(Z_{Lx} + jZ_{Ly})(b_x + jb_y)\}q^2\\&= (Z_{Lx}b_x - Z_{Ly}b_y)q^2\\&= \begin{bmatrix}Z_{Lx} & Z_{Ly}\end{bmatrix}\begin{bmatrix}b_x\\-b_y\end{bmatrix}q^2\end{aligned} \tag{A.7}$$

Denoting p_x and p_y as real and complex parts of $P(j\omega)$, and c_x and c_y as real and imaginary parts of $C(j\omega)$, also as we denoted $C(j\omega)\overline{P}(j\omega) = b_x + jb_y$, b_x and b_y becomes

$$b_x = c_x p_x + c_y p_y \tag{A.8}$$

$$b_y = c_y p_x - c_x p_y \tag{A.9}$$

Thus, the 2 by 1 vector in (A-7) is

$$\begin{aligned}\begin{bmatrix}b_x\\-b_y\end{bmatrix} &= \begin{bmatrix}c_x p_x + c_y p_y\\-c_y p_x + c_x p_y\end{bmatrix}\\&= \begin{bmatrix}c_x & c_y\\-c_y & c_x\end{bmatrix}\begin{bmatrix}p_x\\p_y\end{bmatrix}\end{aligned} \tag{A.10}$$

From (A.7), (A.10), and using the definitions of (10.a)-(10.e), the proof of equality (A.2) is straightforward.

Hyoun-Suk Kim

was born in 1968 in Seoul Korea. He received B.S., M.S. and Ph.D degrees in Mechanical Engineering at KAIST (Korea Advanced Institute of Science and Technology) in 1991, 1993 and 1998, respectively. Currently, he is senior researcher at ETRI (Korea Electronics and Telecommunications Research Institute). He is interested in adaptive signal processing, signal processing for 3D sound reproduction, active noise/vibration control.

Appendix B: proof of $\boldsymbol{S_L H^t C S_L' = U_L Q \Lambda Q^{-1} U_L'}$

Let's consider singular value decomposition of S_L

$$\boldsymbol{S_L = U_L \Sigma_L V_L'} \tag{B.1}$$

where L+1 by 2 matrix $\boldsymbol{U_L}$ and 2 by 2 matrix Σ_L are given in (15.a) and (16.b), while $\boldsymbol{V_L}$ is 2 by 2 rotation matrix as follows

$$\boldsymbol{V_L} = \begin{bmatrix}\cos\frac{1}{2}\omega T & \sin\frac{1}{2}\omega T\\-\sin\frac{1}{2}\omega T & \cos\frac{1}{2}\omega T\end{bmatrix} \tag{B.2}$$

Using the property that $\boldsymbol{V_L}$, $\boldsymbol{H}$ and $\boldsymbol{C}$ are scaled rotation matrices and commutable to each other, the cross-correlation matrix $\boldsymbol{K}$ can be rearranged as

$$\begin{aligned}\boldsymbol{K} &= \boldsymbol{S_L H^t C S_L'}\\&= \boldsymbol{U_L \Sigma_L V_L' H^t C V_L \Sigma_L U_L'}\\&= \boldsymbol{U_L \Sigma_L H^t C \Sigma_L U_L'}\end{aligned} \tag{B.3}$$

There exist invertable matrix $\boldsymbol{Q}$ and diagonal matrix Λ whose diagonal elements are eigenvalues of $\Sigma_L H^t C \Sigma_L$ such that

$$\boldsymbol{\Sigma_L H^t C \Sigma_L = Q \Lambda Q^{-1}} \tag{B.4}$$

where precise expression of $\boldsymbol{Q}$ and Λ are given in (15.b) and (15.c), respectively. Thus, combining (B.3) and (B.4) with variables as in (15) and (16), $\boldsymbol{K}$ is decomposed into $\boldsymbol{U_L Q \Lambda Q^{-1} U_L'}$.

Youngjin Park

was born in 1957 in Seoul, Korea. He received the B.S. degree in Mechanical Engineering and M.S. degree in Mechanical Design in 1980 and 1982, respectively from Seoul National University. He obtained Ph.D degree in Mechanical Engineering from the University of Michigan, Ann Arbor in 1987. From 1988 and 1990, he was an Assistant Professor in the Department of Mechanical Engineering and Industrial Engineering at the New Jersey Institute of Technology. In 1990, he joined the Korea Advanced Institute of Science and Technology, where he is currently an Associate Professor of Mechanical Engineering. His research interests include robust control theory, active noise/vibration control, vehicle dynamics and control, and smart material applications